I4: A New Parallel Mechanism for Scara Motions

Sébastien Krut♣, Olivier Company♣, Michel Benoit♣, Hiromichi Ota♠, François Pierrot♣

(♣)LIRMM, UMR 5506, CNRS - Université Montpellier II
161 rue Ada, 34392 Montpellier cedex 5, France

(♠)TOYODA Machine Works, LTD. - Technical R&D Center
1-1, Asahimachi, Kariya, Aich, Japan

***Abstract* – This paper presents a new robot which produces four motions for high speed handling (three translations and one rotation about a given axis in world coordinates). This machine is an evolution of H4's architecture. Firstly, H4 advantages are recalled, and some limitations are mentioned. To compensate for these limitations a new design of the traveling plate is proposed. A description of the whole mechanism is given. The structure's ability to provide Scara Motions is presented. Geometrical conditions that must be followed in order to obtain desired motions are discussed. Kinematics models are derived. The design of the first prototype is described.**

I. INTRODUCTION

The four dof of Scara motions are well adapted to pick-and-place tasks: three translations to carry an object from one point to another plus one rotation to orientate the object. Pick-and-place applications usually require high speeds and accelerations and the success of machines based on the Delta [1] architecture comes from the fact that their hybrid design (three dof in parallel for the translation, plus one serial rotation) often fit remarkably the industry needs. However, in some cases (namely for Delta with huge workspace, or even more, for linear Delta), the serial ***R****UPU*[1] chain installed between the base and the traveling plate to create the rotational dof may become a machine's weak point.

In recent years, researches have proposed different designs offering Scara motions; some of them are fully-parallel mechanisms, like Kanuk [2] or H4 [3], some others have non-fully-parallel designs [4]. Other four-dof parallel mechanisms had been studied in the past, but they are dedicated to different applications such as Koevermans' flight simulator [5] and Reboulet's four-dof wrist [6].

Recently, prototypes have been built and evaluated, showing that the H4 architecture could offer good performances in pick-and-place applications as well as in handling of heavy loads. Currently, work on calibration and identification are under progress.

All these efforts have pointed out H4's advantages as well as H4's limitations. Starting from these limitations, this paper firstly proposes a new mechanical architecture (called I4) which will keep H4's key features (in-parallel Scara motion, Delta-like construction, high-speed ability, easy design) and in the same time suppress most H4's limitations. Then a section is dedicated to a detailed explanation of I4's motions. Kinematics models are derived, and the design of the first prototype, based on linear motors and new passive joints is described.

[1] Revolute, Universal, Prismatic and Universal joints. Actuation and measurement are usually installed on the revolute joint (***R***), while the other joints are passive and not equipped with sensors (*U*, *P*, *U*).

II. FROM H4 TO I4

It has been shown that H4 is an architecture providing Scara motions applicable to high speed robotics. One specific feature of this architecture is its articulated mobile platform (made with two pivot joints) which is linked to the base by four identical Delta-like "spatial parallelograms" (Fig. 1). This traveling plate can be equipped with an additional gear-based amplification system leading to a large and adjustable range of motion in orientation.

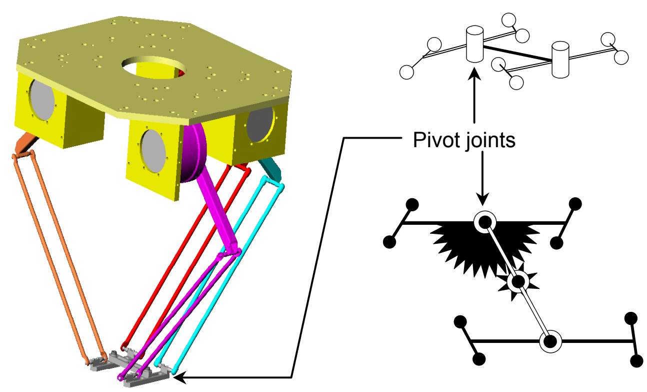

Fig. 1 - H4, the articulated mobile platform and the additional gear-based amplification system

However, some of its limitations can be pointed out:

- When the tool orientation is changed, the Jacobean matrix condition number may vary a lot, leading to important changes in the machine behavior; in the same time, internal collisions may occur, depending on the practical design.
- It has been proved [3] that the relative positions of the four "spatial parallelograms" must be properly selected to avoid singular cases. Specifically, placing them at 90 degrees from each other (as in Fig. 2, left part) is not recommended, while it would have been nice to choose a design symmetrical with respect to the vertical axis for practical matters.
- Its forward geometrical model has not been established in analytical form, except for specific arrangements.

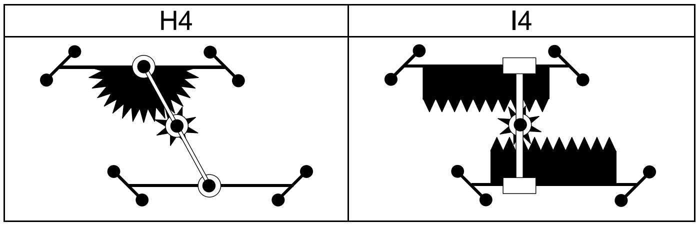

Fig. 2 - H4 and I4 traveling plates.

In this paper, we propose a new mobile platform concept that solves these problems. The basic idea looks simple: replacing the pivots joints by prismatic joints, and gears by rack-and-pinion. Indeed, it is a little more tricky than it seems at first sight, and the following sections will enlighten:

- The fact that such an architecture offers Scara motions;
- The fact that this mechanism is hyper-static (over constrained), and ways to overcome this point;
- The reason for having two rack-and-pinion systems rather than one.

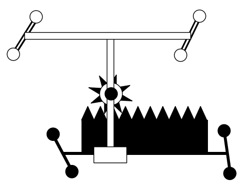

Fig. 3 - Another possibility for I4's traveling plate.

However, one point should be clear already: the risk of self-collision (one part of the traveling plate colliding the other) is drastically reduced. This is also true for another mobile platform design depicted in Fig. 3. Here, only one prismatic joint is kept: the traveling plate is made up of two parts rather than three, but looses its symmetrical design, good for balancing load among the parts.

III. I4 GENERAL CONCEPT

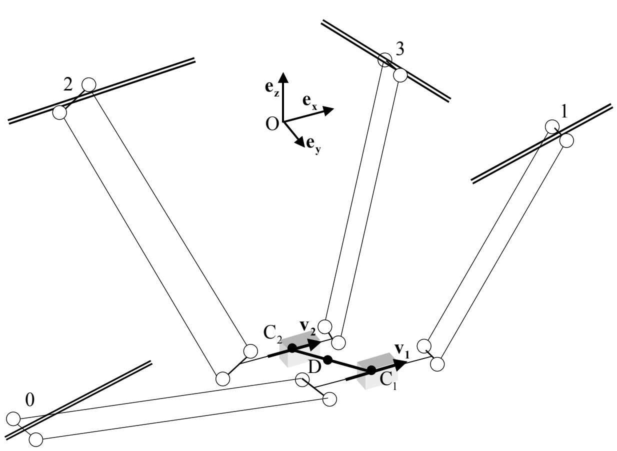

Fig. 4 - I4's structure

This paper focuses on the I4 whose traveling plate corresponds to Fig. 2, right part; the moving platform is made of three parts, two lateral parts, and one central part: each lateral part is connected to two Delta-like "spatial parallelograms" by ball joints, and to the central part by a prismatic joint. As for the Delta or the H4 architecture, the actuators are fixed to the base to reduce moving parts' masses, and are linked to "spatial parallelograms" by ball joints (see Fig. 4). Since I4 belongs to Delta-H4 family, the same remarks hold: motors may be rotational or linear motors, the ball joints may be replaced by U-joints, and so on.

In working conditions both rods in a "spatial parallelogram" $(SS)_2$ (two *SS* chains parallel one to the other) stay in a common plane. This implies that $\mathbf{n_{i1}} = \mathbf{n_{i2}}$ where $\mathbf{n_{ij}}$ is the vector joining A_{ij} to B_{ij} (respectively $\mathbf{n_i}$ joining A_i to B_i), $i \in \{1,2,3,4\}$ (see Fig. 5). Since both rods are considered as plain solids, the impossible motion is the rotation about the vector $\mathbf{n_{i1}} \times \mathbf{u_i}$ where $\mathbf{u_i}$ is the vector joining B_{i1} to B_{i2}.

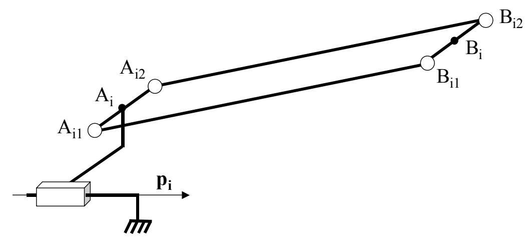

Fig. 5 - *P(SS)₂* chain

In Fig. 6, a joint-and-loop graph is depicted: gray boxes represent actuated joints, white boxes passive joints. Underlined letter stands for a joint equipped with measurement. Circles express a coupling between two joints.

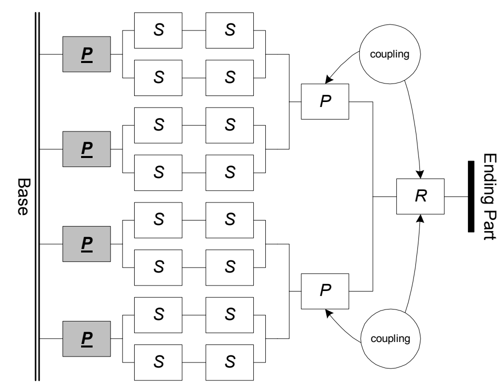

Fig. 6 - I4's joint-and-loop graph

A. Mechanisms Motions

According to Hervé's notations [7] for displacements subgroups, $\{T\}$ stands for the subgroup of spatial translations and $\{X(\mathbf{u})\}$ stands for the subgroup of Schoenflies displacements (that is to say 3 translations and 1 rotation about a given axis with respect to world coordinates), where $\mathbf{u}$ is a unitary vector collinear to the rotation's axis.

If a closed loop mechanism is composed of two chains producing Schoenflies displacements with $\mathbf{v} \neq \mathbf{u}$, then:

$$\{X(\mathbf{u})\} \cap \{X(\mathbf{v})\} = \{T\} \tag{1}$$

that is to say that such a mechanism will produce only three translations.

In working conditions each *P(SS)₂* chain's possible displacement belongs to $\{X(\mathbf{u'_i})\}$ where $\mathbf{u'_i}$ is the unitary vector collinear to $\mathbf{u_i}$ defined in previous section. If $\mathbf{u'_1} \neq \mathbf{u'_2}$, according to equation (1) possible displacements of segment B_0B_1 belong to $\{T\}$ subgroup. The same remark stands also for segment B_2B_3. Because of the prismatic joints linking C_1C_2 to the two former $\{T\}$ subgroup, this ending part belongs also to $\{T\}$ subgroup: that is to say, the end-effecter can translate in all directions relatively to world's coordinates.

B. Geometrical Conditions

In this section we focus on the orientation of vectors $\mathbf{u_i}$ to guarantee a non-singular design for the mechanism. Assuming that $\dot{\mathbf{x}}$ is the velocity of point D, $\boldsymbol{\omega}$ the rotation velocity of the end-effecter, v_1 the linear velocity of C_1C_2 relative to B_0B_1 about $\mathbf{v_1}$ and v_2 the one relative to B_2B_3 about $\mathbf{v_2}$, speed of point B_{ij} can be written as follows:

$$\dot{\mathbf{x}}_{\mathbf{B_{ij}}} = \dot{\mathbf{x}} + \boldsymbol{\omega} \times \mathbf{s_{ij}} + v_k \, \mathbf{v_k} \tag{2}$$

where $\mathbf{s_{ij}}$ is the vector joining D to B_{ij}, with $k=1$ for $i \in \{0,1\}$ and $k=2$ for $i \in \{2,3\}$.

And velocity of point A_{ij} can be written as follows:

$$\dot{\mathbf{x}}_{\mathbf{A_{ij}}} = \dot{q}_i \, \mathbf{p_i} \tag{3}$$

where $\mathbf{p_i}$ is a vector tangent to point A_{ij} trajectory. For linear motors this vector is unitary; for rotational motors, its norm is equal to the distance of point A_{ij} to the rotational axis.

Using a rigid body's velocity properties applied to each bar, the following equations can be written as follows:

$$\mathbf{M_1} \begin{bmatrix} \dot{\mathbf{x}} & \boldsymbol{\omega} & v_1 & v_2 \end{bmatrix}^T = \mathbf{N_1} \dot{\mathbf{q}} \tag{4}$$

where:

$$\mathbf{M_1} = \begin{bmatrix} \mathbf{n_{01}} & \mathbf{s_{01}} \times \mathbf{n_{01}} & \mathbf{v_1 . n_{01}} & 0 \\ \mathbf{n_{02}} & \mathbf{s_{02}} \times \mathbf{n_{02}} & \mathbf{v_1 . n_{02}} & 0 \\ \mathbf{n_{11}} & \mathbf{s_{11}} \times \mathbf{n_{11}} & \mathbf{v_1 . n_{11}} & 0 \\ \mathbf{n_{12}} & \mathbf{s_{12}} \times \mathbf{n_{12}} & \mathbf{v_1 . n_{12}} & 0 \\ \mathbf{n_{21}} & \mathbf{s_{21}} \times \mathbf{n_{21}} & 0 & \mathbf{v_2 . n_{21}} \\ \mathbf{n_{22}} & \mathbf{s_{22}} \times \mathbf{n_{22}} & 0 & \mathbf{v_2 . n_{22}} \\ \mathbf{n_{31}} & \mathbf{s_{31}} \times \mathbf{n_{31}} & 0 & \mathbf{v_2 . n_{31}} \\ \mathbf{n_{32}} & \mathbf{s_{32}} \times \mathbf{n_{32}} & 0 & \mathbf{v_2 . n_{32}} \end{bmatrix}, \quad \mathbf{N_1} = \begin{bmatrix} \mathbf{p_0 . n_{01}} & 0 & 0 & 0 \\ \mathbf{p_0 . n_{02}} & 0 & 0 & 0 \\ 0 & \mathbf{p_1 . n_{11}} & 0 & 0 \\ 0 & \mathbf{p_1 . n_{12}} & 0 & 0 \\ 0 & 0 & \mathbf{p_2 . n_{21}} & 0 \\ 0 & 0 & \mathbf{p_2 . n_{22}} & 0 \\ 0 & 0 & 0 & \mathbf{p_3 . n_{31}} \\ 0 & 0 & 0 & \mathbf{p_3 . n_{32}} \end{bmatrix},$$

$$\dot{\mathbf{q}} = \begin{bmatrix} q_1 & q_2 & q_3 & q_4 \end{bmatrix}^T.$$

(**.** represents the dot product, × the cross product)

Assuming that, when the mechanism is assembled, $\mathbf{n_{i1}} = \mathbf{n_{i2}} = \mathbf{n_i}$, by subtracting equations, system (4) can be written:

$$\mathbf{M_2} \begin{bmatrix} \dot{\mathbf{x}} & \boldsymbol{\omega} & v_1 & v_2 \end{bmatrix}^T = \mathbf{N_2} \dot{\mathbf{q}} \tag{5}$$

with:

$$\mathbf{M_2} = \begin{bmatrix} \mathbf{n_0} & \mathbf{s_{01}} \times \mathbf{n_0} & \mathbf{v_0 . n_0} & 0 \\ \mathbf{n_1} & \mathbf{s_{11}} \times \mathbf{n_1} & \mathbf{v_1 . n_1} & 0 \\ \mathbf{n_2} & \mathbf{s_{21}} \times \mathbf{n_2} & 0 & \mathbf{v_2 . n_2} \\ \mathbf{n_3} & \mathbf{s_{31}} \times \mathbf{n_3} & 0 & \mathbf{v_3 . n_3} \\ \mathbf{0} & \mathbf{u_0} \times \mathbf{n_0} & 0 & 0 \\ \mathbf{0} & \mathbf{u_1} \times \mathbf{n_1} & 0 & 0 \\ \mathbf{0} & \mathbf{u_2} \times \mathbf{n_2} & 0 & 0 \\ \mathbf{0} & \mathbf{u_3} \times \mathbf{n_3} & 0 & 0 \end{bmatrix}, \quad \mathbf{N_2} = \begin{bmatrix} \mathbf{p_0 . n_0} & 0 & 0 & 0 \\ 0 & \mathbf{p_1 . n_1} & 0 & 0 \\ 0 & 0 & \mathbf{p_2 . n_2} & 0 \\ 0 & 0 & 0 & \mathbf{p_3 . n_3} \\ 0 & 0 & 0 & 0 \\ 0 & 0 & 0 & 0 \\ 0 & 0 & 0 & 0 \\ 0 & 0 & 0 & 0 \end{bmatrix}.$$

Noting $\mathbf{M_2} = \begin{bmatrix} \mathbf{M_{21}} \\ \mathbf{M_{22}} \end{bmatrix}$, where $\mathbf{M_{22}}$ is composed by the four last lines of $\mathbf{M_2}$, the following equation is obtained:

$$\mathbf{M_{22}} \begin{bmatrix} \dot{\mathbf{x}} & \boldsymbol{\omega} & v_1 & v_2 \end{bmatrix}^T = \mathbf{0} \tag{6}$$

As all the elements of the three first columns of $\mathbf{M_{22}}$ are equal to zero, $\dot{\mathbf{x}}$ has no influence in equation (6). It's the same for the two columns regarding v_1 and v_2. This leads to an over-determined system (3 unknowns for 4 equations):

$$\mathbf{M_{un}} \boldsymbol{\omega} = \mathbf{0} \tag{7}$$

with :

$$\mathbf{M_{un}} = \begin{bmatrix} \mathbf{u_0} \times \mathbf{n_0} \\ \mathbf{u_1} \times \mathbf{n_1} \\ \mathbf{u_2} \times \mathbf{n_2} \\ \mathbf{u_3} \times \mathbf{n_3} \end{bmatrix}.$$

1) Condition 1

To get only translation motions, $\boldsymbol{\omega}$ must be equal to zero. A necessary condition for this statement is that matrix $\mathbf{M_{un}}$ is of full rank ($rank = 3$). For example, this situation is obtained when considering the constructive disposition with a perfect symmetry of the pairs of rods with respect to a vertical axis as in Fig. 2; for the H4 robot, the same disposition led to a singular configuration.

Note 1. Such an over-determined system expresses the fact that the mechanism is hyper-static (over-constrained). This implies that a constraint may be released: for example making $\mathbf{u_3} = \mathbf{0}$ (a "spatial parallelogram" degenerates into a single rod) leads to an isostatic version of I4. Thus, I4 may be built with three $\underline{\mathbf{P}}(SS)_2$ chains plus one $\underline{\mathbf{P}}$SS chain, for example. Or, it may be built with four $\underline{\mathbf{P}}(SS)_2$ chains if machining and assembly accuracy is sufficient, or if a flexible component is added in the mechanism.

Remark 1. The previous condition is only a *necessary* condition. It has to be verified for all the points of the desired workspace. Singular configurations relative to the actuation are not taken into account in this derivation.

2) Condition 2

Knowing that $\boldsymbol{\omega} = \mathbf{0}$ and considering $\mathbf{M_{21}}$ as the matrix composed of the four first lines of $\mathbf{M_2}$, the following system is obtained:

$$\begin{bmatrix} \mathbf{n_0} & \mathbf{v_0}.\mathbf{n_0} & 0 \\ \mathbf{n_1} & \mathbf{v_1}.\mathbf{n_1} & 0 \\ \mathbf{n_2} & 0 & \mathbf{v_2}.\mathbf{n_2} \\ \mathbf{n_3} & 0 & \mathbf{v_3}.\mathbf{n_3} \end{bmatrix} \begin{bmatrix} \dot{\mathbf{x}} \\ v_1 \\ v_2 \end{bmatrix} = \begin{bmatrix} \mathbf{p_0}.\mathbf{n_0}\ q_0 \\ \mathbf{p_1}.\mathbf{n_1}\ q_1 \\ \mathbf{p_2}.\mathbf{n_2}\ q_2 \\ \mathbf{p_3}.\mathbf{n_3}\ q_3 \end{bmatrix} \tag{8}$$

Note 2. This system is an under-determined system (5 unknowns for 4 equations). To solve it, an additional constraint must be added. In practice by adding rack-and pinion systems, such as in Fig. 2, a coupling between v_1 and v_2 is created ($v_1 = k\ v_2$), and the desired rotational motion is produced.

IV. KINEMATIC MODELING

In this section, relationships between actuators' and traveling plate's positions (represented by $\mathbf{x} = [x \quad y \quad z \quad t]^T$ in frame $\langle \mathrm{O}, (\mathbf{e_x}, \mathbf{e_y}, \mathbf{e_z}) \rangle$) are derived. The relationship between actuators' and traveling plate's velocities, respectively represented by $\dot{\mathbf{q}}$ and $\dot{\mathbf{x}}$, is also presented. We focus here on the specific case where $\mathbf{v_1} // \mathbf{v_2} // \mathbf{e_x}$ (see Fig. 7).

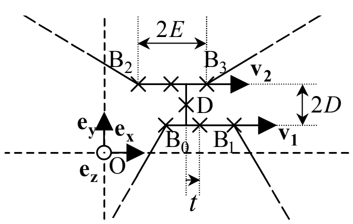

Fig. 7 - Geometrical parameters of the I4's traveling plate

Representative vectors of geometrical points D, $\mathrm{B_0}$, $\mathrm{B_1}$, $\mathrm{B_2}$ and $\mathrm{B_3}$ are written as follows:

$$\mathbf{D} = \begin{bmatrix} x & y & z \end{bmatrix}^T,$$

$$\mathbf{B_0} = \mathbf{D} + \begin{bmatrix} -E+t & -D & 0 \end{bmatrix}^T,\ \mathbf{B_1} = \mathbf{D} + \begin{bmatrix} E+t & -D & 0 \end{bmatrix}^T,$$

$$\mathbf{B_2} = \mathbf{D} + \begin{bmatrix} -E-t & D & 0 \end{bmatrix}^T,\ \mathbf{B_3} = \mathbf{D} + \begin{bmatrix} E-t & D & 0 \end{bmatrix}^T.$$

In this particular case, t is equal to the shift between the central part an both lateral parts of the traveling plate. In practice this is done by using two identical rack-and-pinion systems each side. A simple proportional relationship exist between the orientation angle θ and this parameter: $t = k \times \theta$.

A. Relationship between $\mathbf{x}$ *and* $\mathbf{q}$

1) Inverse Position Relationship

As it is usual for most parallel robots, the inverse position relationship is easy to compute. It is derived from the following equality:

$$\left\| \mathbf{A_i B_i} \right\|^2 = L_i^{\ 2},\ i \in \{0,\ 1,\ 2,\ 3\} \tag{9}$$

The resolution can either be derived for linear motors as well as for rotational motors (see for example in [12]).

2) Forward Position Relationship

A nice feature of I4 is that an analytic position relationship can be derived. Indeed, equation (9) leads to the following 4-equation system:

$$\begin{cases} (x+t)^2 + a_0(x+t) + y^2 + b_0 y + z^2 + c_0 z + d_0 = 0 & (10) \\ (x+t)^2 + a_1(x+t) + y^2 + b_1 y + z^2 + c_1 z + d_1 = 0 & (11) \\ (x-t)^2 + a_2(x-t) + y^2 + b_2 y + z^2 + c_2 z + d_2 = 0 & (12) \\ (x-t)^2 + a_3(x-t) + y^2 + b_3 y + z^2 + c_3 z + d_3 = 0 & (13) \end{cases}$$

Subtracting equation (11) to (10) and (13) to (12) leads to:

$$(x+t) = \frac{(b_1 - b_0)}{(a_0 - a_1)} y + \frac{(c_1 - c_0)}{(a_0 - a_1)} z + \frac{(d_1 - d_0)}{(a_0 - a_1)} \tag{14}$$

$$(x-t) = \frac{(b_3 - b_2)}{(a_2 - a_3)} y + \frac{(c_3 - c_2)}{(a_2 - a_3)} z + \frac{(d_3 - d_2)}{(a_2 - a_3)} \tag{15}$$

When (14) and (15) are merged with (11) and (13), a system composed of 2 quadrics is obtained:

$$\begin{cases} \alpha_{01} y^2 + \beta_{01} y + \chi_{01} z^2 + \delta_{01} z + \varepsilon_{01} = 0 & (16) \\ \alpha_{12} y^2 + \beta_{12} y + \chi_{12} z^2 + \delta_{12} z + \varepsilon_{12} = 0 & (17) \end{cases}$$

Thus the solution is clearly the intersection of two ellipses. The algebraic solutions are known [16], and the proper solution is easy to choose by geometrical considerations. In section 5, a detailed solution will be written for a specific arrangement.

B. Relationship between $\dot{\mathbf{x}}$ *and* $\dot{\mathbf{q}}$

This relationship can be written in the following form, resorting to matrices $\mathbf{J_x}$ and $\mathbf{J_q}$:

$$\mathbf{J_x}\ \dot{\mathbf{x}} = \mathbf{J_q}\ \dot{\mathbf{q}} \tag{18}$$

Indeed, by introducing the 2 matrixes **N** and **N'**:

$$\mathbf{N} = \begin{bmatrix} 1 & 0 & 0 & 1 \\ 0 & 1 & 0 & 0 \\ 0 & 0 & 1 & 0 \end{bmatrix} \text{ and } \mathbf{N}' = \begin{bmatrix} 1 & 0 & 0 & -1 \\ 0 & 1 & 0 & 0 \\ 0 & 0 & 1 & 0 \end{bmatrix},$$

velocities of points B_0, B_1, B_2 and B_3, can be written:

$$\mathbf{V_{B_0}} = \mathbf{V_{B_1}} = \mathbf{N}\ \dot{\mathbf{x}}, \quad (19)$$

$$\mathbf{V_{B_2}} = \mathbf{V_{B_3}} = \mathbf{N'}\ \dot{\mathbf{x}}. \quad (20)$$

To derive equation (18), the classical property relating the velocities, $\mathbf{v}(A_i)$ and $\mathbf{v}(B_i)$, of two points, A_i and B_i, belonging to the same rigid body is used:

$$\mathbf{v}(A_i).\mathbf{n_i} = \mathbf{v}(B_i).\mathbf{n_i} \quad (21)$$

Applying (27) to the four chains leads to:

$$\mathbf{J_x} = \begin{bmatrix} \mathbf{n_0.N} \\ \mathbf{n_1.N} \\ \mathbf{n_2.N'} \\ \mathbf{n_3.N'} \end{bmatrix}, \quad (22)$$

$$\mathbf{J_q} = diag\left(\mathbf{n_i.p_i}\right). \quad (23)$$

($\mathbf{p_i}$ is a vector tangent to point A_i's trajectory, see section III.B for its definition.)

V. PARTICULAR ARRANGEMENT FOR THE I4 ROBOT

In this paper the focus is put on one particular design depicted in Fig. 8, where four linear motors are orientated all in the same direction: this guarantee a huge workspace in a particular direction.

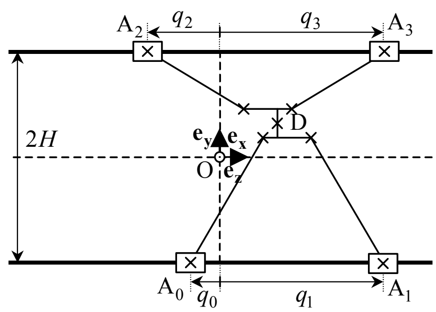

Fig. 8 - I4 geometry, top view

In this particular case $\mathbf{v_1} // \mathbf{v_2} // \mathbf{e_x} // \mathbf{p_i}$, and points A_0, A_1, A_2 and A_3 can be written in frame $\left\langle O,(\mathbf{e_x},\mathbf{e_y},\mathbf{e_z})\right\rangle$ as follows:

$$\mathbf{A_0} = \begin{bmatrix} q_0 \\ -H \\ 0 \end{bmatrix},\ \mathbf{A_1} = \begin{bmatrix} q_1 \\ -H \\ 0 \end{bmatrix},\ \mathbf{A_2} = \begin{bmatrix} q_2 \\ H \\ 0 \end{bmatrix},\ \mathbf{A_3} = \begin{bmatrix} q_3 \\ H \\ 0 \end{bmatrix}.$$

Inverse model is:

$$\begin{cases} q_0 = (x+t) - \left(E + \sqrt{L^2 - z^2 - (y+(H-D))^2}\right) & (24) \\ q_1 = (x+t) + \left(E + \sqrt{L^2 - z^2 - (y+(H-D))^2}\right) & (25) \\ q_2 = (x-t) - \left(E + \sqrt{L^2 - z^2 - (y-(H-D))^2}\right) & (26) \\ q_3 = (x-t) + \left(E + \sqrt{L^2 - z^2 - (y-(H-D))^2}\right) & (27) \end{cases}$$

Methods to obtain forward and inverse geometrical relationships are the one explained in previous sections, but in this case simplifications occur.

Forward model is:

$$\begin{cases} x = \dfrac{(q_0+q_1)+(q_2+q_3)}{4} & (28) \\ y = \dfrac{(q_3-q_2-2E)^2-(q_1-q_0-2E)^2}{16(H-D)} & (29) \\ z = -\sqrt{\begin{matrix} L^2-(H-D)^2-y^2 \\ -1/8\left((q_3-q_2-2E)^2+(q_1-q_0-2E)^2\right) \end{matrix}} & (30) \\ t = \dfrac{(q_0+q_1)-(q_2+q_3)}{4} & (31) \end{cases}$$

For this particular geometry, relations between the vectors directing the bars can be observed:

$$\mathbf{n_0.x} = -\mathbf{n_1.x}, \text{ and } \mathbf{n_0.y} = \mathbf{n_1.y},\ \mathbf{n_0.z} = \mathbf{n_1.z} \quad (32)$$

$$\mathbf{n_2.x} = -\mathbf{n_3.x} \text{ and } \mathbf{n_2.y} = \mathbf{n_3.y},\ \mathbf{n_2.z} = \mathbf{n_3.z} \quad (33)$$

This leads to the particular inverse Jacobean matrix:

$$\mathbf{J_m} = \begin{bmatrix} 1 & \mathbf{n_0.y/n_0.x} & \mathbf{n_0.z/n_0.x} & 1 \\ 1 & -\mathbf{n_0.y/n_0.x} & -\mathbf{n_0.z/n_0.x} & 1 \\ 1 & \mathbf{n_2.y/n_2.x} & \mathbf{n_2.z/n_2.x} & -1 \\ 1 & -\mathbf{n_2.y/n_2.x} & -\mathbf{n_2.z/n_2.x} & -1 \end{bmatrix} \quad (34)$$

Note 3. This matrix exhibits interesting properties directly related to machine performances. One of them is that this matrix depends neither of x nor t. In fact, a movement relative to x or t, does only shift parts of the mobile platform along $\mathbf{x}$. As a consequence, vectors $\mathbf{n_i}$ are independent of those 2 parameters. Moreover, as it can be seen in (34), $\mathbf{J_m}$ only depends of vectors $\mathbf{n_i}$; and corollary is independent of x and t. Thus, the performances of the mechanism (regarding kinetostatic transformations) are independent of the position relative to $\mathbf{x}$ and of the orientation of the ending part.

Such considerations allowed us to consider the optimal design of our first I4 prototype in a rather simple way. We searched for the parameters D, H and L (for practical reasons, D was chosen equal to E) minimizing $\max\left(cond\left(\mathbf{J_m}\right)\right)$ over a workspace defined only along two directions (y range: 400 mm, z range: 200 mm). The parameters values were found to be:

$$D = E = 0.15 \text{ m},\ H = 0.5 \text{ m},\ L = 1 \text{ m}.$$

Of course, the accessible workspace is much larger than the one used for the optimization. Fig. 9 presents the domain where the condition number is smaller than 3 (note that along x direction, the workspace is only limited by the actuators' range)

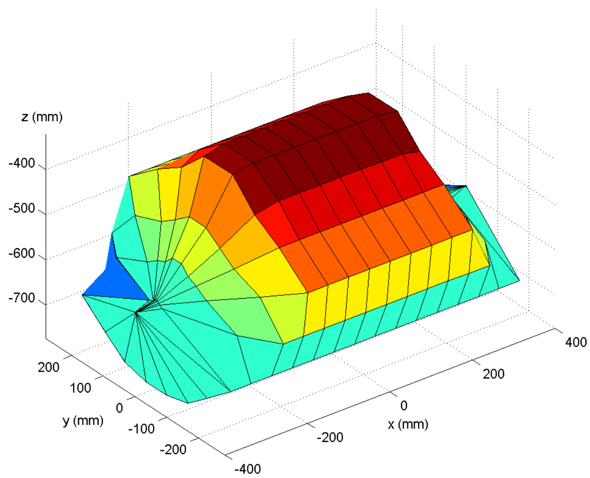

Fig. 9 - I4's workspace for $\text{cond}(\mathbf{J_m})<3$

VI. PROTOTYPE DESIGN

The practical design is extremely simple thanks to Linear motors (Fig. 10). Rods and traveling plate are made of aluminum. Spherical joints are new passive joints made by INA Company (we have verified that no internal singularity for these joints occurs). To reach a ±180 degrees range of motion, the mobile platform has been equipped with two rack-and-pinion systems (Fig. 11).

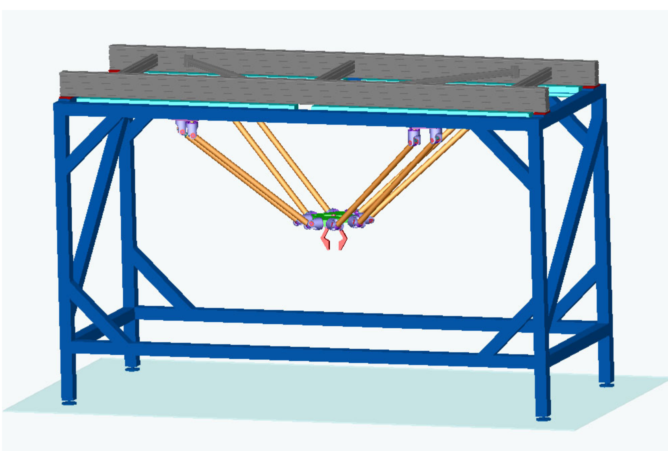

Fig. 10 - CAD view of the I4 prototype

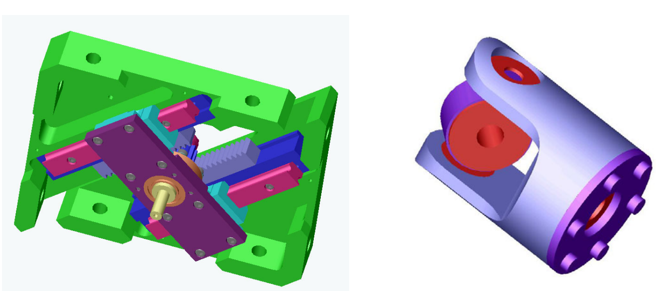

Fig. 11 - I4 traveling plate and INA joint.

VII. CONCLUSION

In this paper a 4 dof parallel robot, based on the H4 architecture, useful for high speed handling, has been proposed. Its new traveling plate succeed in overcoming the H4 limitations. The structure's ability to provide the needed dof has been presented and geometrical conditions necessary to obtain desired motions were established. The design of practical arrangement and its kinematics models have been discussed. One key point is the derivation of Jacobean matrix which explains the good behavior of this se mechanism. A prototype is currently under construction and patents are pending for I4 machines.

VIII. REFERENCES

[1] R. Clavel, "Une nouvelle structure de manipulateur parallèle pour la robotique légère", *APII*, 23(6), 1965, pp. 371-386.

[2] Rolland L., "The Manta and the Kanuk: Novel 4 dof parallel mechanism for industrial handling", *in Proc. of ASME Dynamic Systems and Control Division IMECE'99 Conference*, Nashville, USA, November 14-19, 1999, vol. 67, pp 831-844.

[3] Pierrot F., Company O., "H4: a new family of 4-dof parallel robots", *in Proc of IEEE/ASME International Conference on Advanced Intelligent Mechatronics*, Atlanta, Georgia, USA, September 19-22, 1999, pp. 508-513.

[4] Angeles J., Morozov A., Navarro O., "A novel manipulator architecture for the production of SCARA motions", *in Proc. IEEE International Conference on Robotics and Automation*, San Francisco, April 24-28, 2000, pp. 2370-2375.

[5] Koevermans W.P. *et al.*, "Design and performance of the four dof motion system of the NLR research flight simulator", *in Proc. of AGARD Conf.*, No 198, Flight Simulation, La Haye, 20-23 October 1975, pp. 17-1/17-11.

[6] Reboulet C. *et al*, "Rapport d'avancement projet VAP", thème 7, phase 3. Rapport de Recherche 7743, CNES/DERA, January 1991.

[7] Hervé J.M., "The Lie group of rigid body displacements, a fundamental tool for mechanism design", *Mechanism and Machine Theory*, Vol. 34, 1999, pp. 719-730.

[8] Furuya N., Soma K., Chin E., Makino, "Research and development of selective compliance assembly robot arm. II. Hardware and software of SCARA controller", *Journal of the Japan Society of Precision Engineering/Seimitsu Kogaku Kaishi*, Vol. 49, n°7, 1983, pp. 835-841.

[9] Pierrot F., Dauchez P. and Fournier A., "Fast parallel robots", *Journal of Robotic Systems*, 8(6), 1991, pp. 829-840.

[10] Hesselbach J., Plitea N., Frindt M., et Kusiek A., "A new parallel mechanism to use for cutting convex glass panels", *in ARK*, Strobl, June 29-July 4, 1998, pp. 165-174.

[11] Tanev T.K., "Forward displacement analysis of a three legged four-degree-of-freedom parallel manipulator", *in ARK*, Strobl, June 29-July 4, 1998, pp. 147-154.

[12] Merlet J.-P. and Pierrot F., "Modélisation des robots parallèles", in *Analyse et modélisation des robots manipulateurs*, Lavoisier, ISBN 2-7462-0300-6, 2001, pp. 93-144.

[13] Hervé J.M., "Analyse structurelle des mécanismes par groupes de déplacements", *Mechanism and Machine Theory*, Vol. 13, 1978, pp. 437-450.

[14] Company O., Pierrot F., "A new 3T-1R parallel robot", *in Proc. of 9th International Conference on Advanced Robotics*, Tokyo, Japan, October 25-27, 1999, pp. 557-562.

[15] Pierrot F., Marquet F., Company O., Gil T., "H4 parallel robot: modeling, design and preliminary experiments", *in Proc. of IEEE Int. Conf. On Robotics and Automation*, Seoul, Korea, May 2001.

[16] Eberly D., "Intersection of Ellipses", Magic Software Inc., 6006 Meadow Run Court, Chapel Hill, NC 27516, USA.